Applied Acoustics 198 (2022) 108986

Contents lists available at ScienceDirect

Applied Acoustics

journal homepage: www.elsevier.com/locate/apacoust

Scaling laws for unmitigated pile driving: Dependence of underwater noise on strike energy, pile diameter, ram weight, and water depth

Jonas von Pein [a,*], Tristan Lippert [b], Stephan Lippert [a], Otto von Estorff [a]

[a] Hamburg University of Technology, Institute of Modelling and Computation, Denickestrasse 17, 21073 Hamburg, Germany
[b] AQUSTIX GbR, Katharinenstrasse 4, 20457 Hamburg, Germany

ARTICLE INFO

Article history:
Received 17 January 2022
Received in revised form 22 July 2022
Accepted 13 August 2022
Available online 27 August 2022

Keywords:
Pile driving
Underwater noise
Scaling laws finite element model

ABSTRACT

Sound produced by marine pile driving activities poses a possible risk to marine life. The assessment and mitigation of this risk requires a prediction of the expected sound levels. While different analytical models have been presented to estimate the decay characteristics of pile driving noise, the estimation of the source level still requires the use of numerical modelling in most cases. The paper at hand discusses the possibilities and limits of estimating approximate source or any other levels by scaling laws, using measurement data from previous projects. The identified main influencing factors include strike energy of the hammer, pile diameter, ram weight, and water depth. The scaling laws are derived from theoretical considerations verified against results of a state-of-the-art finite element model for pile driving noise radiation. The found dependencies are then validated against a set of offshore measurement results. It is shown that the obtained scaling laws provide an option to approximately estimate the sound exposure levels of pile driving activities from one site to the other, within practical ranges of accuracy.

1. Introduction

Driven piles are currently the most widely used foundation technique for offshore wind turbines. The piling process can lead to relatively high sound levels within the water, reaching levels at which the marine fauna is potentially affected. Mammals like whales, harbour porpoises, dolphins, and seals as well as fish and other aquatic life in the ocean can change their behaviour due to the high sound levels, cf. Kasteleien et al. [1], Halvorsen et al. [2], and Schaffeldt et al. [3].

To protect the marine environment, limiting values have to be fulfilled in many regions of the world. See e.g. Müller and Zerbs [4] for the German regulations, National Marine Fisheries Service [5] for the guidelines of the USA, and Skjellerup et al. [6] for the rules in Denmark and the corresponding guidelines [7]. In order to estimate whether the limits will be fulfilled, precise prognosis tools are necessary. There are various numerical models which have been developed for this purpose, see for example Reinhall and Dahl [8], Zampolli et al. [9], Tsouvalas and Metrikene [10], Fricke and Rolfes [11], Lipppert and von Estorff [12], Lippert et al. [13], and von Pein et al. [14].

An overview and comparison of existing pile driving noise models is given in the description of the results of the pile driving noise benchmarks COMPILE I and II by Lippert et al. [15–17]. A detailed review of existing approaches to model pile driving noise was recently given by Tsouvalas [18].

While currently providing the most precise results, numerical models have the drawback of being only accessible to a limited number of experts. Furthermore, a lot of input parameters are necessary that may not exist at an early stage of the planning phase. Often empirical models are used in practice to reduce time and the need for complex modelling. However, these models are once again only available to few people with access to a decent data base and do not take detailed pile geometries, the hammer types, and the specific soil layering into account. Therefore, the authors believe that an option for estimating sound levels that is open to a wider range of users and requires less precise input data is useful for an initial assessment of the need for noise mitigation systems and the impact of the sound levels on the marine fauna.

There are a number of analytical models to compute the sound levels at various distances. The damped cylindrical spreading model (DCS) developed by Lippert et al. [19] has shown to be in reasonable accordance with measurement values up to 5 km. Usually, the limitations and therefore the measurements are defined and conducted in ranges of up to 2 km. The DCS has also been used by Heaney et al. [20] and validated for mitigated scenarios by Jestel

* Corresponding author.
E-mail address: jonas.pein@tuhh.de (J. von Pein).

https://doi.org/10.1016/j.apacoust.2022.108986
0003-682X/

et al. [21]. However, the DCS as well as other spreading laws rely on a reference sound level at a certain range as a key input parameter. This could either be a source level at 1m or a measurement value at any other distance. This paper is intended to close the gap of the inevitably necessary source values for the analytical propagation models by scaling existing measurement data. It is focussed on the scaling of the single-strike sound exposure level (SEL). Often, other quantities such as the zero-to-peak pressure level SPL_{peak} are also of interest. Once the SEL is derived, the SPL_{peak} can be approximated by the approach developed by Lippert et al. [22] and applied in Ainslie et al. [23].

As the case where a precise level for a location of interest is already existing seems of limited practical reference to the authors, the dependence of the SEL on the considered parameters are of great interest for assessing the influence of changes of the pile driving scenario. Based on this, existing noise levels from previous pile driving activities which are openly available can be used as the input parameter for future sites, for which the SELs are to be assessed.

This paper is organized as follows: In section 2 the used numerical model is briefly described. The derivation of the scaling laws is shown within section 3. There, the main influencing parameters are identified, the numerical results of their variation are shown, and the physics behind the derived scaling law is explained. The scaling laws are verified against two models with different soil set-ups and penetration depths in section 4 and validated with a variety of mostly publicly available measurement data sets at distances of around 750 m in section 5. Finally, the applicability of the results and their general limits in light of the high number of used approximations are discussed and an outlook on future work is given.

2. Numerical Model

The numerical model used in the following is based on the finite element method (FEM), see Heitmann et al. [24]. An extensive validation of the modelling approach is shown by von Pein et al. [14] for three scenarios with and without noise mitigation measures.

The FEM model is set up as rotationally symmetric, using a central difference time integration scheme. Within the model the pile, the water, and the soil are discretized and coupled with each other. The soil is assumed to be of layered linear-elastic material. At the sea-surface a zero-pressure boundary condition is used and a mixed Dirichlet–Neumann boundary condition is applied at the outer range of the water domain. To prevent artificial reflections at the radial and lower end of the linear-elastic soil, infinite elements are used. Within the embedded part of the pile Rayleigh damping is induced, which is determined to be equivalent to the losses of plastic deformation, friction, and other loss mechanisms between pile and soil. The pile head excitation is computed within a pre-calculation, which separately considers the interaction of the different parts of the hammer with the pile. The computed pile head excitation is afterwards applied as a boundary condition at the pile top within the acoustical model. In general, the model can include computed or measured excitation signals.

The outcome of the model is the pressure time series $p(t)$. The single-strike SEL, also often referred to as $L_{E,p}$, is defined by

$$\mathrm{SEL} = 10\log_{10}\left(\frac{E_p}{E_{p0}}\right)\left(\mathrm{dBre1}\,\mu\mathrm{Pa^2s}\right), \tag{1}$$

with the sound exposure defined by $E_p = \int_{t_1}^{t_2} p^2(t)\,\mathrm{dt}$ and the reference value $E_{p0} = 1\,\mu\mathrm{Pa^2s}$. The times t_1 and t_2 are the beginning and end of the sound event [25].

3. Derivation of scaling laws

In the following, the main influencing parameters identified in this study are presented, varied within the FEM model, and the resulting influences on the SEL are discussed.

3.1. Discussion of main influencing parameters

The resulting SELs at every piling location are influenced by the interaction of various factors. These are among others: the acoustical properties and the layering of the soil, the hammer configuration, the strike energy, the pile geometry, the penetration depth, the bathymetry, the general sea state, and the use of noise mitigation measures.

The main influencing parameters, which are usually available with measurement reports and can be estimated for future pile driving scenarios, are believed to be: strike energy E, pile diameter d, water depth h_w, and the ram weight m_r, based on the assessment of measurement reports from various sites as well as numerical modelling runs. Therefore, the authors have chosen to investigate the influence of these parameters in the following to derive approximate scaling laws for pile driving noise estimations for monopiles covering the full water column.

The influence of a submerged pile head could be included in the scaling laws by considering the quotient of wetted pile length L_w and water depth h_w in $\Delta\mathrm{SEL}_{L_w} = k\log_{10}(L_w/h_w)$ with $k = 8.3$ according to Lippert et al. [13].

An initial assessment of the influence of the layering and the acoustical properties of the soil has been made by Lippert and von Estorff [12]. Even though the soil has to be taken into account for a detailed pile driving noise prognosis, it is not possible to generalize the soil within a simple scaling law. Furthermore, especially the acoustical soil properties are usually not publicly available and often unknown at an early stage of the planning phase. Therefore, and being fully aware of the strong simplification this represents, the bottom structure is assumed to consist of an infinite half space rather than a layered structure for the scaling in the following.

The chosen hammer configuration also influences the SEL. However, the influence of the hammer configuration with hammer, pile guide, follower, and anvil is hard to generalize. Simplifying, only the ram weight is taken into consideration in the following, giving the best trade-off between capturing the effects of different hammers, while still allowing general conclusions.

This paper focuses on the SEL at distances close to the pile up to 750 m. For distances further away, e.g., greater than 5 km, the influence of frequency dependent propagation loss needs to be reassessed.

Furthermore, only unmitigated pile driving scenarios have been considered in the following to demonstrate the basic applicability of the identified dependencies.

3.2. Parameter variation using the numerical model

The FEM model and especially the soil layering represent a typical North Sea bottom, based on the site of Bard Offshore 1 [26,14]. The evaluation of the influence of the strike energy, diameter, and ram weight is done by comparing the differences between the SEL computed with the depth-averaged sound exposure at 20 m from the pile center. In order to show the influence of the water depth, the SEL is evaluated at 750 m distance.

The variation of the piling energies is performed with a fully cylindrical pile having an outer diameter of 4 m and a constant wall thickness of 0.1 m. All other parameters were the same as in Table 2. The strike energy is varied from 500 kJ to 8000 kJ, representing the lower range of currently used driving energies in prac-

tice up to piling energies above the potential of hydraulic hammers currently in development. This is achieved by varying the vertical pile head velocity profile $v(t)$ consisting of half a sine wave defined for the time length T

$$v(t) = -\hat{v}\sin\left(\frac{t}{T}\pi\right). \tag{2}$$

The corresponding strike energy can be computed with the pile head impedance Z by

$$E = Z\int_0^T v^2(t)\,\mathrm{d}t. \tag{3}$$

The amplitude $\hat{v}$ is derived by scaling Eq. 2 to the correct strike energy and the pile head impedance is defined with the Young's Modulus of steel E_s, the cross sectional area of the pile head A_p, and the longitudinal wave speed of the pile c_p as $Z = \frac{E_s\,A_p}{c_p}$. The energy variation is conducted with $T = 8$ms.

In order to compute the influence of the outer diameter of the pile on the SEL, the diameter is varied between 2 m and 12 m, representing a realistic upper limit for pile sizes currently in development. Once again the velocity profile $v(t)$ from Eq. 2 is used, which is scaled such that the strike energy is 2000 kJ in every case. Model runs have been performed with different time lengths T of the pile head excitation leading to different excitation frequency spectra.

In order to verify the influence of the ram weight m_r on the SEL, the velocity profile at the pile head is computed with the analytical formula provided by Deeks and Randolph [27] in which the anvil properties are neglected. The pile head velocity $v(t)$ is defined in dependence on the pile head impedance, the initial velocity of the ram v_0, and the ram weight m_r by

$$v(t) = v_0\exp(-Z/m_r\,t). \tag{4}$$

The initial velocity of the ram is derived out of its kinetic energy E by $v_0 = \sqrt{2\,E/m_r}$.

The influence of the water depth on the SEL is computed with the same model as the energy variation, despite a constant strike energy of 2000 kJ and a pile length of 105m. Furthermore, model runs are also conducted with a homogeneous soil, in order to have a defined reflection coefficient R between water and soil. The homogeneous soil has been considered with a compressional wave speed of 1750ms^{-1}, a shear wave speed of 150ms^{-1}, and a density of 1800kg m^{-3}.

3.3. Discussion of dependencies

The results of the FEM model runs are compared by evaluating the difference ΔSEL of the SEL at a certain position. The SEL is computed with the depth averaged sound exposure E_p, compare Eq. 1. The observed dependencies have been evaluated at several different ranges and have been found to be independent of the evaluation range in first approximation. The resulting relations of the differences of the SEL are defined with a reference value indicated by the subscript 0 and the target value indicated by the subscript i.

3.3.1. Strike energy

The resulting differences of the computed SELs 20 m away from the pile center are shown in Fig. 1 for the variation of the strike energy. An increase of the strike energy directly leads to an increase of the acoustical energy. Assuming a linear dependence of the acoustical energy on the strike energy, the difference $\Delta\mathrm{SEL}_E$ derived with different energies E can be computed by

$$\Delta\mathrm{SEL}_E = 10\log_{10}(E_i/E_0). \tag{5}$$

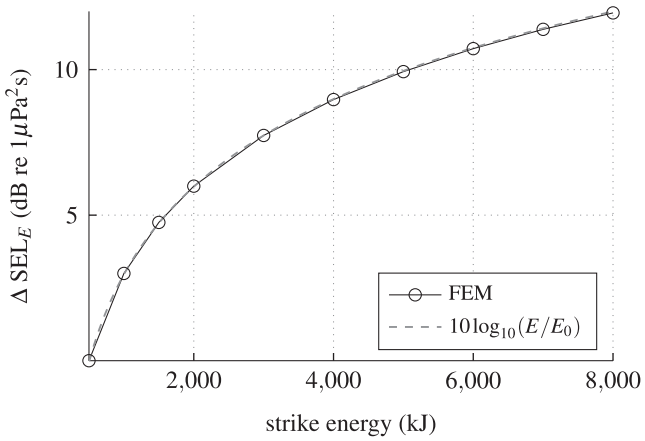

Fig. 1. The differences between the computed SEL at a range of 20 m over the considered strike energies together with the $10\log_{10}(E/E_0)$ results scaled from E_0 = 3000 kJ.

This relation is also shown within Fig. 1 and it agrees well with the computed SELs. In real-life the contact behaviour between the pile and the different parts of the hammer changes non-linearly. However, the resulting discrepancy is assumed to be rather small in the operating range of a hammer and object of further research. Despite the non-linear influence of the hammer components, there is no limit in the application of the found dependency, given a practical range of input parameters is used. From measurement data Bellmann et al. [46] derived an increase of 2.5 dB to 3 dB per doubling of strike energy, which is equivalent to factors of 8.3 and 10 in Eq. 5.

3.3.2. Diameter

The results of the diameter variation are displayed in Fig. 2. The dependence of the SEL on the diameter has been found to be an interplay of various main influencing factors. Considering a rod, the radial expansion is linearly increasing with the radius, if the stress is kept constant [28]. As the radial deformation of the pile and the sound pressure in the water are linked, the SEL would increase by $\Delta\mathrm{SEL}_d = 20\log_{10}(d_i/d_0)$. However, the pile head excitation is scaled such that the energy is kept constant, therefore, the stress is decreasing, c.f. Eqs. (2) and (3). As can bee seen in Fig. 2, the influence of the diameter is depending on the pile head excitation $v(t)$ and therefore the frequency spectrum of the pile head excitation. With increasing diameter the ring frequency defined by

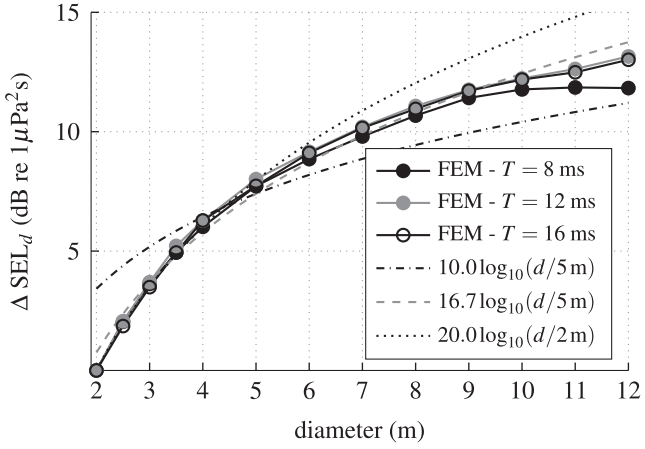

Fig. 2. The differences between the computed SEL at a range of 20 m over the considered diameters computed with time lengths T together with two trend lines.

$$f_r = \frac{1}{\pi d}\sqrt{\frac{E}{\rho}} \tag{6}$$

decreases. Tsouvalas [29] showed that the frequency content of the pile head excitation below the ring frequency is amplified and transmitted to the sound pressure waves. The energy content in frequencies above the ring frequency is not as well transmitted. These findings are also in accordance with Szechenyi [30], who states that the radiation efficiency is increasing up to the ring frequency f_r. In order to show, which of the used pile head excitations are comparable to the pile head dynamics induced by real-life hammers, the normalized frequency spectrum of the pile head excitations are shown in Fig. 3. Furthermore, the measured normalized spectra of Bard Offshore 1 (BO1) and Global Tech I (GTI) as well as the normalized spectra computed with the FEM for Borkum Riffgrund 1 (BR1) and the COMPILE II benchmark scenario (CPII) are plotted therein. All spectra are normalized with respect to their maximal amplitude. The spectrum of BR1 agrees very well with the $v(t)$ derived with $T = 8$ ms. The comparison of BO1, GTI, and CPII with the generically derived pile head excitations also show a good agreement. This comparison indicates that the pile head excitations derived with T between 8ms and 16ms result in spectra that are similar to the measured and computed spectra of real-life hammers. Reconsidering Fig. 2, a best-fit approximation with a least-squares approximation of the $T = 12$ ms results and $d_0 = 5$ m leads to $k = 16.7$. for

$$\Delta\mathrm{SEL}_d = k\log_{10}(d_i/d_0). \tag{7}$$

3.3.3. Ram weight

The results of the differences between the SEL computed with different ram weights are displayed in Fig. 4. The pile head excitation from Eq. 4 leads to a dependence of the SEL on the ram weight according to

$$\Delta\mathrm{SEL}_{m_r} = 10\log_{10}(m_{r,0}/m_{r,i}). \tag{8}$$

This way of modelling the influence of the ram weight on the SEL is neglecting the influence of a changing stiffness of the ram weight and anvil with changing hammer model or dimensions. The influence of the stiffness of the different hammers cannot easily be generalized. The relation of Eq. 8 is used for the ram weight scaling in the following.

3.3.4. Water depth

The results of the SEL with different water depths at 750 m are shown in Fig. 5. Therein the SEL averaged over the water depth at

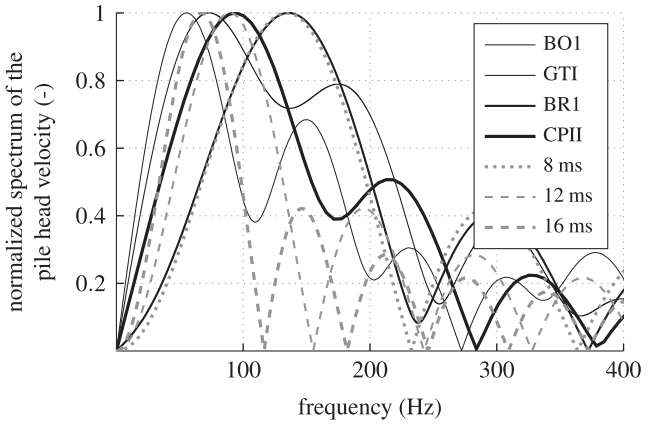

Fig. 3. The normalized spectrum of the pile head velocities used in Fig. 2 and the measured pile head velocities of BO1 and GTI as well as the spectra of the computed pile head velocities of BR1 and CPII.

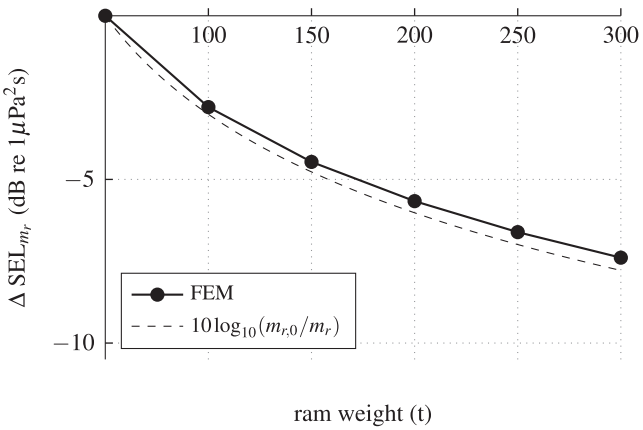

Fig. 4. The differences between the computed SEL at a range of 20 m over the considered ram weights together with the $10\log_{10}(m_{r,0}/m_{r,i})$ results scaled from $m_{r,0}$ = 50t.

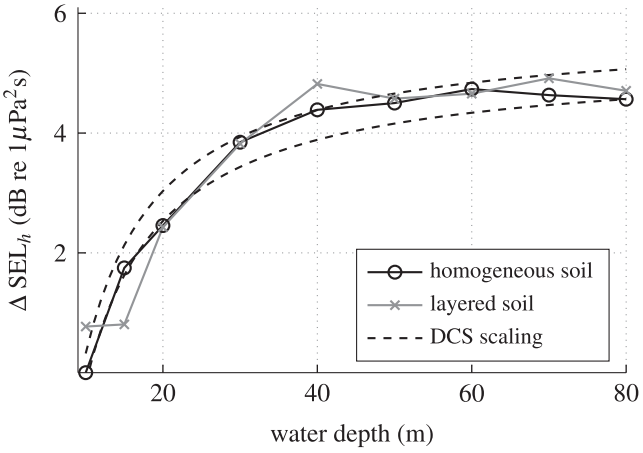

Fig. 5. The differences between the computed SEL at a range of 750 m over the considered water depths with DCS scaling.

750 m computed with two different soil setups is displayed. As expected, the results of the homogeneous soil are much smoother than the ones derived with the layered soil profile.

The dependence of the SEL on the water depth can be approximated by the DCS, as described by Lippert et al. [19]. Within Fig. 5 two DCS scalings are plotted with different reference water depths. Comparing the two DCS plots a maximum difference of 0.5 dB can be observed. The difference of the SEL at the same distance r_i can be approximated with the reflection coefficient R, the water depth h, and the propagation angle φ by

$$\Delta\mathrm{SEL}_h = \left(\frac{10\log_{10}\left(|R_i|^2\right)}{2\cot(\varphi)h_i} - \frac{10\log_{10}\left(|R_0|^2\right)}{2\cot(\varphi)h_0}\right) r_i. \tag{9}$$

The propagation angle φ is approximately 17° as shown by Reinhall and Dahl [8] and the reflection coefficient can be computed with the acoustical parameters of the soil and water, c.f. Tindle and Zhang [31]. The FEM model is run with a homogeneous soil with an approximated reflection coefficient of $|R_0| = 0.947$, computed with damping factors of 0.6 dB per wavelength for the compressional wave and 3.5 dB per wavelength for the shear waves.

It is important to notice, that the lower range of the validity of the DCS scaling of the influence of the water depth is valid only when the main acoustical energy content is above the cut-off fre-

quency of the considered wave guide. The cut-off frequency depends on the soil conditions and the water depth [32].

4. Verification of scaling laws

So far the discussed dependencies have all been discussed separately, to explain the underlying characteristics and physical mechanisms. However, the authors believe that varying a single parameter is of limited use in practice. To scale results from one site to another, for almost all cases, more than one of the identified main influencing factors will be different. This is even more so, if several existing sites are to be scaled to the same parameters of interest, to be able to do a statistical evaluation.

From a theoretical point of view, a linear sum over the different influencing factors does not hold. However, for the present application case, this seems to be a practical approach, within the specified (and very narrow) range of parameters. This is believed to result on the one hand from partly linear behavior within the specified ranges, and on the other hand from the to a first degree decoupled effects of the four key quantities. In this light, the authors believe that practical gain in terms of accessibility to a wide range of users outweighs the error that is induced here. However, this always has to be kept in mind and any further extension of the range of applicability would have to be tested for validity first.

The expected overall difference ΔSEL_{scaled} between two scenarios is computed the following way:

$$\Delta SEL_{scaled} = 10\log_{10}\left(\frac{E_1}{E_0}\right) + 16.7\log_{10}\left(\frac{d_1}{d_0}\right) - 10\log_{10}\left(\frac{m_{r,1}}{m_{r,0}}\right) + 750\frac{10\log_{10}\left(|R|^2\right)}{2\cot(\varphi)}\left(\frac{1}{h_1}-\frac{1}{h_0}\right). \quad (10)$$

As one tangible example to demonstrate that the found dependencies can be added up linearly within certain limits using the formula derived above, two very different models are used.

The first model is set up using a water depth of 20 m, a pile diameter of 3 m, a strike energy of 500 kJ, and the geometry of the MHU 1900S hammer with a ram weight of 95t.

The second model is set up with a water depth of 40m, a pile diameter of 6.6m, a strike energy of 3500 kJ, and the MHU 3500S hammer with a ram weight of 175t. Within both scenarios a pile length of 80 m and a wall thickness of 0.1 m is used.

The models are run with the penetration depths of 15, 25, and 35 m and with four different soil setups, based on the locations used in von Pein et al. [14] as well as the soil conditions of the COMPILE II scenario [16], resulting in 12 different combinations.

All scenarios are run by the FEM model described in section 2 and the difference between the numerical results is compared to the theoretical difference ΔSEL_{scaled}. With the reflection coefficient $|R| = 0.971$ the expected difference for all 12 combinations is $\Delta SEL_{scaled} = 12.2$dB.

Within Table 1 the computed SEL at 750 m averaged over the water depth and the according ΔSEL_{FEM} are listed. Therein it can be seen, that ΔSEL_{scaled} is in the range of the ΔSEL_{FEM} with a minimal difference of 0.2 dB and a maximal difference of 0.9 dB. Furthermore, the influence of the different soil profiles is in a range of 1 dB.

The dependence of the SEL on the penetration depth for these cases could be conservatively estimated by $\Delta SEL_{pen} = -0.75$ dB/10m.

The results of this verification indicate, that, at least to a first approximation, the influence of the different factors can be summed up independently. The main source of uncertainty is, in this case, the interplay of the pile and the different hammers.

Summarizing, once an unmitigated sound level is available for a specific hammer set up, pile design, and a particular soil profile, the derived scaling laws can be used e.g. to estimate the impact of changes of the considered parameters.

5. Validation of scaling laws

Next, the derived scaling laws are validated against measurement data sets. First, the origin of the values and the characteristics of the piling location are described. Second, the SELs of the different piling locations are scaled and the resulting differences are compared.

5.1. Data used for the validation

For sites where a detailed measurement report is available a single-strike SEL has been chosen with the according strike energy. Otherwise, the so called SEL_{05} is used which is a statistical measure of the occurring SEL with only 5% of the strikes being higher than that. It is assumed, that the highest levels occur at final penetration with the highest strike energy.

During the BORA project [26], three measurement campaigns were conducted in the North Sea at Bard Offshore 1 (BO1), Global Tech I (GTI), and Borkum Riffgrund 1 (BR1) [34–35].

For BO1 the measured SEL at 745 m of the second reference measurement is considered with a measured SEL of 177 dB [33].

For GTI it is important to point out that the pile head was submerged during the whole piling process (tripod foundation). The closest measurement distance was 583 m and a measurement value of an early piling stage with the pile head close to the sea surface is used in the following [35].

The measurement results and case description of the real-life pile driving noise modelling benchmark COMPILE II (CPII) are also considered even though they have the drawback of a sea floor with a gradual slope [16].

The results of a pile driven in the Anholt wind farm (AN) in the Baltic Sea are taken from Lippert and von Estorff [12]. The AN scenario is considered with an SEL of 169.7 dB.

The measurement data of Horns Rev II (HRII) as presented by Brandt et al. [36] are also taken into account.

Five similar piles were driven into the sea floor at Hornsea (HS) [37]. In the following, the mean of the five measured SEL of 179 dB scaled to the averaged strike energy of 2300 kJ is used. The lowest measured SEL was 2.4 dB lower and the highest was 2.1 dB higher.

Furthermore, measurement results from the German part of the North Sea, namely Amrumbank West (AW) [38], Borkum West II (BW2) [39], and Butendiek (BU) [40] are used together with the results from Prinses Amaliawindpark (PA) [41] and the results of three different piles from the Gemini (GE) [42] wind farm from the Dutch part of the North Sea.

The SEL considered in the following for AW is the mean of three different measurement directions at 750 m and is 175.8 dB, c.f. table 9 in Stein et al. [38]. For the comparison of BW2 to the other measurement locations the averaged value of table 1.10 Diederichs et al. [39] of 170 dB at 750 m is used. The SEL around 750 m for PA has been taken from figure 55 and 56 from de Jong [41] and is 172 dB.

The only data set not collected within the North or Baltic Sea is conducted in the USA at test monopiles within the Coastal Virginia Offshore Wind (CV) project [43].

Furthermore, data sets provided by the platform Marine Ears [44] are included. These data sets consist out of the SEL_{05} and the highest strike energy. The data of Sandbank (SB), Arkona (AR), Veja Mate (VM), Albatross (AL), Trianel (TR), and Deutsche Bucht (DB) are taken from Marine Ears [44].

Table 1
The computed SEL at 750 m averaged over the water depth of the different scenarios computed with four different soil profiles and three different penetration depths.

soil profile	model	(dB re $1\mu Pa^2s$)	penetration depth 15m	25m	35m
	scaling	ΔSEL_{scaled}	12.2	12.2	12.2
B01	model 1	SEL	170.4	169.1	168.4
	model 2	SEL	183.0	182.2	181.3
		ΔSEL_{FEM}	12.6	13.1	12.9
GTI	model 1	SEL	171.2	169.6	168.9
	model 2	SEL	183.2	182.3	181.7
		ΔSEL_{FEM}	12.0	12.7	12.8
BR1	model 1	SEL	170.5	169.6	169.0
	model 2	SEL	182.7	182.0	181.1
		ΔSEL_{FEM}	12.2	12.4	12.1
CPII	model 1	SEL	170.2	169.1	168.7
	model 2	SEL	182.9	182.0	181.2
		ΔSEL_{FEM}	12.7	12.9	12.5

Table 2
Details of the piling configurations used for the validation.

wind farm name	SEL $\left(\text{dB re } 1\mu Pa^2s\right)$	range (m)	strike energy (kJ)	pile diameter (m)	water depth (m)	ram weight (t)	hammer type	foundation type	pile length (m)	penetration depth (m)	wall thickness of pile (mm)
HRII	176	720	850	3.9	12	60	Hydrohammer S-1200	monopile		21	
PA	172	750	800	4	22	95	MHU 1900S	monopile	54		25
AN	169.7	750	350	5	18	100	Hydrohammer S-2000	monopile	45	29	
BR1	175*	738	800	5.9	27	100	Hydrohammer S-2000	monopile	58	22	50
BU	173	750	740	6	20	100	Hydrohammer S-2000	monopile	53		
AW	175.8	750	1140	6	20	95	MHU 1900S	monopile	55		
CPII	174.2	750	1525	6.5	39	175	MHU 3500S	monopile	75	30	100
GE2	180.5	677	894	6.6	30	100	Hydrohammer S-2000	monopile	63.4	28.4	
SB	180*	762	1540	6.8	30	175	MHU 3500S	monopile			
GE1	182	732	1486	7	34	100	Hydrohammer S-2000	monopile	66.5	27.5	
AR	181*	748	2500	7.5	24	200	Hydrohammer S-4000	monopile			
VM	178*	744	1820	7.8	39	200	Hydrohammer S-4000	monopile			
CV	173.5	750	687	7.8	24	150	Hydrohammer S-3000	monopile			
AL	182*	745	3160	8	39.8	150	Hydrohammer S-3000	monopile			
TR	176*	749	1550	8	30.5	150	Hydrohammer S-3000	monopile			
DB	178*	749	1760	8	39	200	Hydrohammer S-4000	monopile			
HS	179*	750	2300	8.1	32	200	Hydrohammer S-4000	monopile			
BW2	170	750	1200	2.44	30	60	Hydrohammer S-1200	tripod	40	30	40–60
GE3	170.2	921	400	2.44	35	69	Hydrohammer S-1400	jackett	58.4	23.4	
GTI	173	583	710	2.48	40	66	MHU 1200S	tripod	46.5	15	55
BO1	177*	745	1400	3.36	40	95	MHU 1900S	tripile	85	34.6	75

* marked SEL values are the SEL_{05}

The SELs and corresponding details on the scaling parameters as well as parameters that are to date not easily scalable, e.g., the hammer type, are listed in Table 2. In general, the data sets consist mainly of pile driving scenarios from the North and Baltic Sea at which the piles were driven with the pile head above or close to the sea surface. Typically, the North and Baltic Sea sites can be considered as relatively flat. Therefore, the assumption of a constant water depth is used. Only hammers of the companies MENCK and IQIP are contained within the data set.

5.2. Validation

In the following the scaling law:

$$SEL_i = SEL_0 + 10\log_{10}\left(\frac{E_i}{E_0}\right) + 16.7\log_{10}\left(\frac{d_i}{d_0}\right) - 10\log_{10}\left(\frac{m_{r,i}}{m_{r,0}}\right) + 750\frac{10\log_{10}\left(|R|^2\right)}{2\cot(\varphi)}\left(\frac{1}{h_i} - \frac{1}{h_0}\right) \quad (11)$$

is used. In order to estimate the relative accuracy of Eq. 11, the previously listed measurement results are scaled with the parameters from the HS site as an example. In a first step, all SELs are scaled to the range of 750 m by applying the DCS model. The DCS scaling as well as the water depth scaling is conducted with the same reflection coefficient for all sites. As Lippert et al. reached a good agreement with the DCS model for the SELs measured at BO1, GTI, and BR1, the same material parameters for sand are used to compute R [19]. They have initially been taken from Ainslie [45]. This approach represents a further simplification, as obviously each site has different conditions. The reflection coefficient is computed with the speed of sound of 1500 ms^{-1} and the density 1025 kg m^{-3} of water, the compressional wave speed in the soil 1790 ms^{-1}, and the according density 2140 kg m^{-3}. Neglecting the influence of shear waves and using a grazing angle of 16.9°, the reflection coefficient is $|R| = 0.971$.

In Fig. 6 the differences between the scaled and measured results for the HS scenario are displayed. The mean of the difference is 0.5 dB with a standard deviation of 2.0 dB. Since five measurements are available from the HS site, the minimum and maximum of these are indicated with the error bar. It can be seen, that the results of CPII and TR are underestimating the measured SEL and the results of GE3 and BO1 are resulting in the highest estimate. Possible reasons for that could be that BO1 was built on a tripile with an uncommonly long pile at an early stage of awareness and acoustical optimization of pile driving activities. GE3 is a pin pile for a jacket structure. Bellmann et al. [46] reported that pin piles for jacket structures are usually about 2 dB louder, than comparable mono piles. The major reason for that are presumably coupling effects of the jacket structure, though a detailed scientific analysis of the described effects still has to be carried out, as far the authors are aware. The CPII pile has the highest wall thickness. Still, it cannot be identified which of these factors is the most important for the comparably low SEL of CPII and TR.

In order to validate the found dependencies, three of the four scaling terms in Eq. 11 are applied and the according scaled result is plotted over the unscaled parameter. This is once again done for HS as a random example and shown together with the according scaling law in Fig. 7. In all four plots the scaling law has the same trend as the scaled results. The difference between the upper and lower trend lines is between 7.1 dB and 7.4 dB within each subplot. It can be seen, that the diameter has the highest influence on the SEL, which is also due to the parameter space. The trends of the diameter, strike energy as well as the ram weight agree very well. The influence of the water depth is comparably low and seems to be neglectable. This finding motivated the above choice of a constant bottom assumption across all sites, as the influence of the reflection coefficient was even smaller, when realistic bottom parameters were assumed. It has to be added that the relative effect of the water depth, is depending on the range of interest.

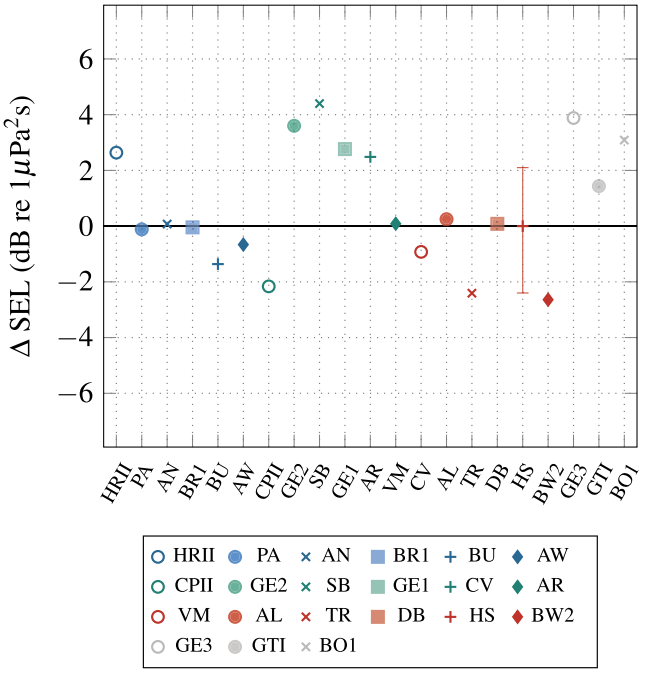

Fig. 6. The difference between the measured and scaled results of the SEL at 750 m for all piling locations, scaled with the parameters of HS.

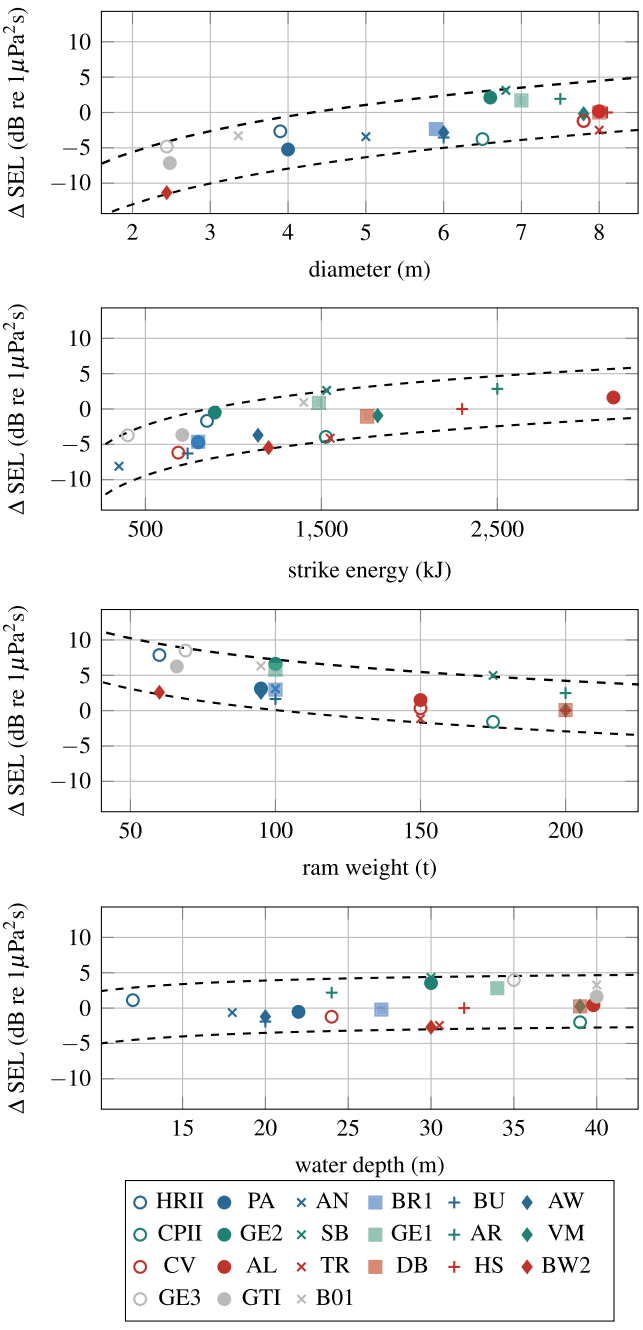

Fig. 7. The mean deviation of the scaled and measured SEL at 750 m over the unscaled quantity together with its lower and upper bound of the scaling law of the unscaled parameter.

For ranges above 750 m, the water depth influence can become dominating.

Another way to demonstrate the influence of each parameter is to show the mean SEL of all data sets listed in Table 2 compared to the measurements with and without the application of the found dependency. The results of the averaged SEL compared to the measured SEL is shown in Fig. 8. Therein it can be seen, that the diameter and strike energy are the most relevant for the presented measurement data. This is also due to the previously mentioned ranges of the data sets, in which the ΔSEL_E and ΔSEL_d are higher than ΔSEL_{m_r} and ΔSEL_h. The initial mean of the deviation is reduced from 4.6 dB to 3.3 dB by the diameter scaling. The consideration of *d*-*E*-scaling leads to a slightly higher mean deviation of 3.4 dB. However, it is also obvious that the energy scaling is necessary, e.g., for the AN scenario. The consideration of the water depth is leading together with *d*-*E*-scaling to a mean deviation of 3.5 dB. Finally, the consideration of the influence of the ram weight together with *d*-*E*-*h*-scaling reduces the mean deviation to 2.5 dB.

6. Discussion

To assess whether the chosen parameters of Eq. 11 represent the data well and are not biased by other effects the equation

$$\mathrm{SEL}_i = \mathrm{SEL}_0 + k_{E,\mathrm{fit}}\log_{10}\left(\frac{E_i}{E_0}\right) + k_{d,\mathrm{fit}}\log_{10}\left(\frac{d_i}{d_0}\right) + k_{m_r,\mathrm{fit}}\log_{10}\left(\frac{m_{r,i}}{m_{r,0}}\right) + k_{h_w,\mathrm{fit}}\left(\frac{1}{h_i}-\frac{1}{h_0}\right) \tag{12}$$

is used for a nonlinear regression [47]. It is performed with the parameters of the HS site. The regression results lead to $k_{E,\mathrm{fit}} = 9.8$, $k_{d,\mathrm{fit}} = 15.3$, $k_{m_r,\mathrm{fit}} = -11.3$, and $k_{h_w,\mathrm{fit}} = -33.7$. The agreement for the energy, diameter, and ram weight with the previously derived trends is very good. Furthermore, the water depth factor which can be computed to $k_{h_w} = -29.1$ from Eq. 11 and the $k_{h_w,\mathrm{fit}}$ are also very consistent. All in all, the regression results show a good agreement with the found scaling laws.

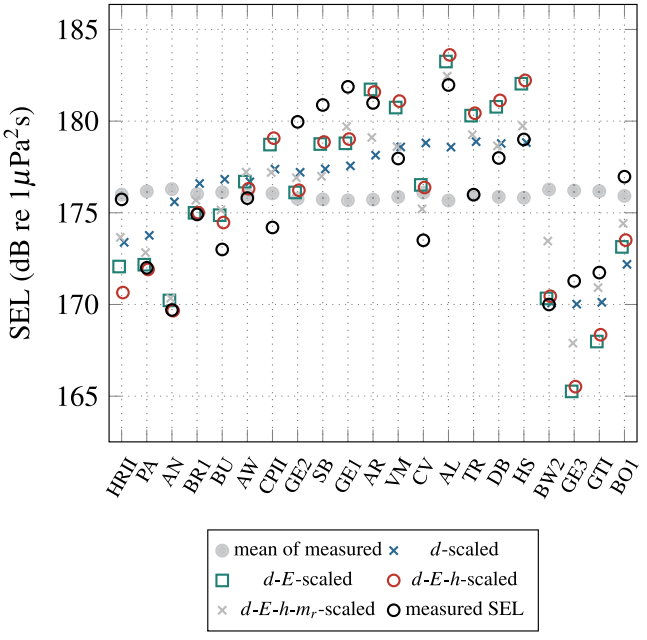

Fig. 8. Comparison of the mean of the measured SEL and the mean of the scaled results with the consideration of different parameters with the actual measured SEL at 750 m for all sites.

The application of the scaling laws depicted in Fig. 6 shows that the absolute difference between the minimum and maximum measured value of the SEL scaled to the 750m position could be reduced from 12.3 dB to 7.0 dB. Furthermore, the results in Fig. 7 indicate, that the identified scaling trends are well reproduced by the measurements. The results of the application of the scaling laws have always to be regarded with the measurement uncertainty, that can have margins of $\pm 2 - 3$dB [14]. A similar margin is also indicated by the range of the measured results of five nominally almost identical piles of HS as presented in Fig. 6. This means that the margin of error of the presented formula is actually comparable in magnitude to the inter-site variation of a single wind farm.

The following effects are believed by the authors to be the main factors, leading to the remaining deviation of up to 7.0 dB: The acoustical parameters of the soil have an influence on the resulting SEL, c.f. Lippert and von Estorff [12]. Furthermore, the geometry of the pile as well as the interplay between chosen hammer configuration and pile also influence the resulting SEL. Finally, the weather and measurement conditions as well as coupling effects between pile and, e.g., a jacket structure affect the measurement results.

To address these factors at least in part and derive a scaling of the SEL of a pile driving set-up for practical examples, two approaches would be suggested by the authors: Either only a small number of very similar piling set-ups is chosen and scaled, or a large variety of results is used and averaged.

To demonstrate the above, two tangible examples will be given. The SEL of the AN site is the lowest of the available mono pile data sets in Table 2 and the SEL of GE1 the highest. These two sites are considered in the following.

The AN and AR site are the only measurement results from the Baltic Sea. Scaling the SEL of AR to AN, leads to a reduction of the initial difference of 11.3 dB to an overestimation of 2.4 dB. The initial difference is computed with the mean of the SELs of the considered data set scaled with the DCS to a range of 750m. Scaling and averaging all available data sets leads to an overestimation of the SEL of 0.6 dB instead of the initial difference of 6.6 dB. If only scenarios with monopiles are considered and averaged, the overestimation of the SEL is also reduced from initially 7.5 dB to 0.5 dB whilst the authors are aware that this is a 'lucky shot', it demonstrates the underlying idea.

Scaling all available data sets with the parameters of GE1 leads to a reduction of the underestimation from 6.2 dB to 2.2 dB. Considering only monopiles reduces the initial underestimation from 5.4 dB to 2.4 dB.

Another possibility is to consider only measurements conducted with the same hammer type. Considering only the measured results of the other five locations at which also the Hydrohammer S-2000 hammer was used leads to a reduction of the initial underestimation from 7.5 dB to 2.2 dB for GE1 and to a reduction of the overestimation from 7.7 dB to 1.2 dB for the AN site.

The according results with the used data set are listed together with the minimal and maximal difference Δ in Table 3.

All in all, the derived scaling laws indicate how the SEL should be corrected with a change in the four parameters. However, the baseline prediction SEL_0 still needs to be derived either by measurements or a numerical model. Therefore, the scaled result will always be biased by the base line prediction or measurement error.

The found scaling laws are believed to be applicable within the considered parameter ranges. Since the biggest simplifications were made in the ram weight variation runs, the choice of a similar hammer type is one way to possibly improve the estimation. Furthermore, it is important to consider sites with similar penetration depths and soil conditions, even though, these are not always known and easily assessed.

Table 3
Comparison of different scaling results. The Δ_{s-m} stands for the difference between the measured and scaled results of the SEL.

	ref data	$\overline{SEL}$	Δ_{s-m}	max Δ_{s-m}	min Δ_{s-m}	comment
AN	all	170.4	0.6	4.3	-2.7	
AN	HRII PA BR1 BU AW CPII GE2 SB GE1 AR VM CV AL TR DB HS	170.2	0.5	4.3	−2.5	monopiles
AN	BR1 BU GE2 GE1	170.9	1.2	3.5	−1.4	Hydrohammer S-2000
AN	AR	172.1	2.4			Baltic Sea
GE1	all	179.7	−2.2	1.6	−5.4	
GE1	HRII PA AN BR1 BU AW CPII GE2 SB AR VM CV AL TR DB HS	179.5	−2.4	1.6	−5.2	monopiles
GE1	AN BR1 BU GE2	179.7	−2.2	0.8	−4.1	Hydrohammer S-2000

7. Conclusion and Outlook

The idea of the paper at hand was to derive dependencies of the SEL on strike energy, diameter, ram weight, and water depth that are relatively easy to apply and can be used for scaling measured or computed SELs from one project to the other. They have been shown to be usable within practical ranges of accuracy, especially if the measurement uncertainties are taken into account. The scaling should be performed over either a small number of very similar piling situations or over a bigger data set and according averaging. The remaining differences of the scaled SELs cannot be related to a single factor but are an interplay of multiple factors such as soil layering and the acoustical properties of the soil, pile geometry, and chosen hammer configuration. Detailed numerical models are, at least to some extend, able to take these parameters into account.

Despite the fact that the general trends of the identified scaling laws could be verified by numerical simulations and validated against offshore measurements, the limitations of the presented approach have to be underlined here again. First, only a very limited number of influencing parameters has been included. Furthermore, the varied range of parameters is relatively small and the found dependencies are only applicable within the range of these limits. This is especially true for the linear summation over practically non-linear phenomena. Finally, the underlying data sets, though quite extensive given the available data at all, is limited to a very narrow geographical region. Therefore the authors would like to emphasize again that the aim of the presented analytical scaling was not to develop a precise model, but a general tool for a broad group of users, providing sound general trends and first estimations.

Especially in early design stages or for initial environmental impact assessments, when detailed data is not available, scaling laws are a meaningful tool for a first estimate of the SELs that are to be expected. Using Eq. 11, the limits of the data set used for the validation need to be kept in mind. These are, e.g., the majority of the considered data is from the North and Baltic Sea. However, the reference data set can be quickly adjusted whenever new measurement data of other locations is available.

The next step will be to identify and validate the derived scaling laws for scenarios including noise mitigation. Another important aspect is, if the found dependencies of the SEL on the diameter and energy can be extrapolated above the range of the existing data set, as suggested. Furthermore, the influence of the non-linear contact behavior of the different hammer parts and therefore the ratio of the strike energy and the maximum possible strike energy of the used hammer will be investigated.

Declaration of Competing Interest

The authors declare that they have no known competing financial interests or personal relationships that could have appeared to influence the work reported in this paper.

Acknowledgments

The authors would like to thank the industrial partners Ørsted Wind Power A/S, EnBW, and MENCK for their support and the fruitful cooperation.

References

[1] Kastelein RA, Gransier R, Marijt MAT, Hoek L. Hearing frequency thresholds of harbor porpoises (Phocoena phocoena) temporarily affected by played back offshore pile driving sounds. J Acoust Soc Am 2015;137:556–64.
[2] Halvorsen MB, Casper BM, Woodley CM, Carlson TJ, Popper AN. Threshold for onset of injury in chinook salmon from exposure to impulsive pile driving sounds. PLoS ONE 2012;7:2–12.
[3] Schaffeld T, Schnitzler JG, Ruser A, Woelfing B, Baltzer J, Siebert U. Effects of multiple exposures to pile driving noise on harbor porpoise hearing during simulated flights - An evaluation tool. J Acoust Soc Am 2020;147:685–97.
[4] Müller A, Zerbs C. Offshore Wind Farms Prediction of Underwater Sound Minimum Requirements on Documentation Technical Report. Hamburg, Germany: Federal Maritime and Hydrographic Agency (BSH); 2013.
[5] National Marine Fisheries Service, 2018 Revision to: Technical Guidance for Assessing the Effects of Anthropogenic Sound on Marine Mammal Hearing (Version 2.0) (2018) 167.
[6] Skjellerup P, Maxon CM, Tarpgaard E, Thomsen F, Schack HB, Tougaard J, Teilmann J, Madsen KN, Mikaelsen MA, Heilskov NF, Marine mammals and underwater noise in relation to pile driving - Working Group 2014 - Report to the Danish Energy Authority, Technical Report July, Esbjerg, Danmark, 2015.
[7] Energistyrelsen, Guideline for underwater noise - Installation of impact-driven piles, Technical Report, Energistyrelsen, Copenhagen, Danmark, 2016.
[8] Reinhall PG, Dahl PH. Underwater Mach wave radiation from impact pile driving: Theory and observation. J Acoust Soc Am 2011;130:1209–16.
[9] Zampolli M, Nijhof MJJ, de Jong CAF, Ainslie MA, Jansen EHW, Quesson BAJ. Validation of finite element computations for the quantitative prediction of underwater noise from impact pile driving. J Acoust Soc Am 2013;133:72–81.
[10] Tsouvalas A, Metrikine AV. A semi-analytical model for the prediction of underwater noise from offshore pile driving. J Sound Vib 2013;332:3232–57.
[11] Fricke MB, Rolfes R. Towards a complete physically based forecast model for underwater noise related to impact pile driving. J Acoust Soc Am 2015;137:1564–75.
[12] Lippert T, von Estorff O. The significance of parameter uncertainties for the prediction of offshore pile driving noise. J Acoust Soc Am 2014;136:2463–71.
[13] Lippert S, Huisman M, Ruhnau M, von Estorff O, van Zandwijk K. Prognosis of Underwater Pile Driving Noise for Submerged Skirt Piles of Jacket Structures. In: Proceedings of the UACE 2017 4th Underwater Acoustics Conference and Exhibition, Skiathos, Greece.
[14] von Pein J, Lippert S, von Estorff O. Validation of a finite element modelling approach for mitigated and unmitigated pile driving noise prognosis. J Acoust Soc Am 2021;149:1737–48.
[15] Lippert S, Nijhof M, Lippert T, Wilkes D, Gavrilov A, Heitmann K, Ruhnau M, von Estorff O, Schäfke A, Schäfer I, Ehrlich J, MacGillivray A, Park J, Seong W, Ainslie MA, De Jong C, Wood M, Wang L, Theobald P. COMPILE - A Generic Benchmark Case for Predictions of Marine Pile-Driving Noise. IEEE J Oceanic Eng 2016;41:1061–71.
[16] Lippert S, von Estorff O, Nijhof MJJ, Lippert T, COMPILE II - A Benchmark of Pile Driving Noise Models against Offshore Measurements, in: Proceedings of Inter-Noise 2018, Chicago, USA, 2018.
[17] Lippert S, von Estorff O. Offshore pile driving noise: Capability of numerical prediction models and ways to consider new technologies, in. In: Town Cape, Africa South, editors. Proceedings of the 7th International Conference on Structural Engineering, Mechanics and Computation.
[18] Tsouvalas A. Underwater noise emission due to offshore pile installation: A review. Energies 2020;13.
[19] Lippert T, Ainslie MA, von Estorff O. Pile driving acoustics made simple: Damped cylindrical spreading model. J Acoust Soc Am 2018;143:310–7.
[20] Heaney KD, Ainslie MA, Halsvorsen M, Seger K, Müller R, Nijhof MJJ, Lippert T, A Parametric Analysis and Sensitivity Study of the Acoustic Propagation for Renewable Energy Sources, Technical Report, U.S. Department of the Interior, Bureau of Ocean Energy Management Prepared by CSA Ocean Sciences Inc. OCS Study BOEM 2020–011, Sterling (VA), 2020.

[21] Jestel J, von Pein J, Lippert T, von Estorff O. Damped cylindrical spreading model: Estimation of mitigated pile driving noise levels. Appl Acoust 2021;184:108350.
[22] Lippert T, Galindo-Romero M, Gavrilov AN, von Estorff O. Empirical estimation of peak pressure level from sound exposure level. Part II: Offshore impact pile driving noise. J Acoust Soc Am 2015;138:EL287–92.
[23] Ainslie MA, Halvorsen MB, Müller RAJ, Lippert T. Application of damped cylindrical spreading to assess range to injury threshold for fishes from impact pile driving. J Acoust Soc Am 2020;148:108–21.
[24] Heitmann K, Mallapur S, Lippert T, Ruhnau M, Lippert S, von Estorff O, Numerical determination of equivalent damping parameters for a finite element model to predict the underwater noise due to offshore pile driving, in: Proceedings of EuroNoise 2015, Maastricht, Netherlands, 2015, pp. 605–610.
[25] DIN ISO18406:2018-08 - Underwater acoustics - Measurement of radiated underwater sound from percussive pile driving (ISO 18406:2017), Technical Report, International Organization for Standardization, Geneva, Switzerland, 2018.
[26] A. Chmelnizkij, O. von Estorff, J. Grabe, E. Heins, K. Heitmann, S. Lippert, T. Lippert, M. Ruhnau, K. Siegl, T. Bohne, T. Grießmann, R. Rolfes, J. Rustemeier, C. Podolski, W. Rabbel, D. Wilken, Schlussbericht des Verbundprojektes BORA: Entwicklung eines Berechnungsmodells zur Vorhersage des Unterwasserschalls bei Rammarbeiten zur Gründung von OWEA (Final Report of the Research Project BORA: Development of a Prediction Model for Underwater Noise, Technical Report, Hamburg University of Technology - Institute of Modelling and Computation, Institute of Geotechnical Engineering and Constrcution Management; Leibniz University Hannover - Institute of Structural Analysis; Kiel University - Christian-Albrechts-Universität, 2016. URL:https://www.tuhh.de/t3resources/bora/layout01INSTITUTE/PDF/BORA_Abschlussbericht-BMWi-FKZ0325421.pdf.
[27] Deeks AJ, Randolph MF. Analytical modelling of hammer impact for pile driving. Int J Numer Anal Meth Geomech 1993;17:279–302.
[28] Möser M, Kropp W, Körperschall, 3 ed., Springer Berlin Heidelberg, Berlin, Heidelberg, 2010. URL:http://link.springer.com/10.1007/978-3-540-49048-7. doi: 10.1007/978-3-540-49048-7.
[29] Tsouvalas A, Underwater noise noise generated by offshore pile driving, November, Delft, The Netherlands, 2015. doi: 10.4233/uuid:55776f60-bbf4-443c-acb6-be1005559a98.
[30] Szechenyi E. Modal densities and radiation efficiencies of unstiffened cylinders using statistical methods. J Sound Vib 1971;19:65–81.
[31] Zhang ZY, Tindle CT. Improved equivalent fluid approximations for a low shear speed ocean bottom. J Acoust Soc Am 1995;98:3391–6.
[32] Jensen FB, Kuperman WA, Porter MB, Schmidt H. Computational Ocean Acoustics. New York, NY: Springer New York; 2011. https://doi.org/10.1007/978-1-4419-8678-8. URL:http://link.springer.com/10.1007/978-1-4419-8678-8.
[33] Bellmann MA, Gündert S, Remmers P, Offshore Messkampagne 1 (OMK1) für das Projekt BORA im Windpark BARD Offshore 1 (Offshore measurement campaign 1 (OMK1) for the BORA project at the wind farm BARD Offshore 1), Technical Report, 2014. URL:https://www.tuhh.de/t3resources/bora/layout01INSTITUTE/PDF/itap_OMK1.pdf.
[34] Bellmann MA, Gündert S, Remmers P, Offshore Messkampagne 2 (OMK2) für das Projekt BORA im Offshore-Windpark Global Tech I (Offshore measurement campaign 2 (OMK2) for the BORA project at the wind farm Global Tech I), Technical Report, 2015a. URL:https://www.tuhh.de/t3resources/bora/layout01INSTITUTE/PDF/itap_OMK2.pdf.
[35] Bellmann MA, Gündert S, Remmers P, Offshore Messkampagne 3 (OMK3) für das Projekt BORA im Offshore-Windpark Borkum Riffgrund 01 (Offshore measurement campaign 3 (OMK3) for the BORA project at the wind farm Borkum Riffgrund 01), Technical Report, 2015b. URL:https://www.tuhh.de/t3resources/bora/layout01INSTITUTE/PDF/itap_OMK3.pdf.
[36] Brandt MJ, Diederichs A, Betke K, Nehls G. Responses of harbour porpoises to pile driving at the Horns Rev II offshore wind farm in the Danish North Sea. Mar Ecol Prog Ser 2011;421:205–16.
[37] Verfuss UK, Bellmann MA, Kühler R, Remmers P, Plunkett R, Underwater noise monitoring during monopile installation at the Hornsea Project One Offshore Windfarm. Report number SMRUC-GOB-2018-012 provided to GoBe Consultants & Ørsted, September 2018, Technical Report September 2018, 2018.
[38] Stein P, Sychla H, Bruns B, Kuhn C, Gattermann J, Stahlmann J, Evaluierung von zwei gemeinsam eingesetzten Schallminderungsmaßnahmen (HSD und BBC) bei den Monopile-Gründungen im OWP Amrumbank West - Untersuchung der Schallkopplungen zwischen Pfahl, Boden und Wasser (Evaluation of two jointly implemented noise reducti, Technical Report, Braunschweig, 2016. doi: 10.2314/GBV.
[39] Diederichs A, Pehlke H, Nehls G, Bellmann M, Gerke P, Oldeland J, Grunau C, Witte S, Rose A, Entwicklung und Erprobung des Großen Blasenschleiers zur Minderung der Hydroschallemissionen bei Offshore-Rammarbeiten (Development and testing of the Big Bubble Curtain to reduce hydro-acoustic emissions during offshore pile driving), Technical Report, Husum, 2014.
[40] Holst H, Bellmann MA, Offshore wind farm Butendiek Construction monitoring Marine mammals Hydro sound measurements (Offshore- Windpark Butendiek Baumonitoring Marine Säuger Hydroschallmessungen), Technical Report, 2014.
[41] de Jong C, Ainslie M, Underwater sound due to piling activities for Prinses Amaliawindpark, Technical Report, TNO, The Hague, 2012.
[42] Remmers P, Bellmann MA, Ecological monitoring of underwater noise during piling at Offshore Wind Farm Gemini (2015) 1–145.
[43] Brinkkemper J, Coastal Virginia Offshore Wind - Noise monitoring during monopile installation A01 and A02, Tech. rep. (2020).
[44] MarinEARS - Marine Explorer and Registry of Sound; specialist information system for underwater noise and national noise-register for the notification of impulsive noise events in the German EEZ of the North- and Baltic Sea to the EU according to the MSFD, 2021. URL:https://marinears.bsh.de.
[45] Ainslie M. Principles of Sonar Performance Modelling. Berlin, Heidelberg: Springer Berlin Heidelberg; 2010. https://doi.org/10.1007/978-3-540-87662-5. arXiv:arXiv:1011.1669v3. URL:http://link.springer.com/10.1007/978-3-540-87662-5.
[46] Bellmann MA, May A, Wendt T, Gerlach S, Remmers P, Underwater noise during the impulse pile-driving procedure: Influencing factors on pile-driving noise and technical possibilities to comply with noise mitigation values. Supported by the Federal Ministry for the Environment, Nature Conservation and Nuclear Safety, Technical Report, 2020.
[47] Seber GA, Wild CJ, Nonlinear Regression, New Jersey, United States of America, 2003.